

Optical breakdown of multilayer thin-films induced by ultrashort pulses at MHz repetition rates

Ivan B. Angelov,^{1,*} Maximilian von Pechmann,² Michael K. Trubetskov,^{1,3}
Ferenc Krausz,^{1,2} and Vladimir Pervak^{2,4}

¹Max-Planck-Institut für Quantenoptik, Hans-Kopfermann-Str. 1, 85748 Garching, Germany

²Ludwig-Maximilians-Universität München, Am Coulombwall 1, 85748 Garching, Germany

³Research Computing Center, Moscow State University, Leninskie Gory, 119992 Moscow, Russia

⁴Ultrafast Innovations GmbH, Am Coulombwall 1, 85748 Garching, Germany

*ivan.angelov@mpq.mpg.de

Abstract: Multilayer coatings composed of TiO₂, Ta₂O₅, HfO₂, or Al₂O₃ as high-index materials and SiO₂ as low-index material were investigated for laser-induced damage using 1 ps, 5 μJ pulses generated by a mode-locked Yb:YAG thin-disk oscillator operating at a wavelength of 1030 nm and repetition rate of 11.5 MHz. Previously reported linear band gap dependence of damage threshold at kHz repetition rates was confirmed also for the MHz regime. Additionally, we studied the effect of electric field distribution inside of the layer stack. We did not observe any significant influence of thermal effects on the laser-induced damage threshold in this regime.

©2013 Optical Society of America

OCIS codes: (140.3330) Laser damage; (310.6870) Thin films, other properties; (320.7090) Ultrafast lasers.

References and links

1. J. Jasapara, A. Nampoothiri, W. Rudolph, D. Ristau, and K. Starke, "Femtosecond laser pulse induced breakdown in dielectric thin films," *Phys. Rev. B* **63**(4), 045117 (2001).
2. M. Mero, J. Liu, W. Rudolph, D. Ristau, and K. Starke, "Scaling laws of femtosecond laser pulse induced breakdown in oxide films," *Phys. Rev. B* **71**(11), 115109 (2005).
3. M. Jupé, L. Jensen, A. Melninkaitis, V. Sirutkaitis, and D. Ristau, "Calculations and experimental demonstration of multi-photon absorption governing fs laser-induced damage in titania," *Opt. Express* **17**(15), 12269–12278 (2009).
4. A. Melninkaitis, T. Tolenis, L. Mažulė, J. Mirauskas, V. Sirutkaitis, B. Mangote, X. Fu, M. Zerrad, L. Gallais, M. Commandré, S. Kičas, and R. Drazdys, "Characterization of zirconia- and niobia-silica mixture coatings produced by ion-beam sputtering," *Appl. Opt.* **50**(9), C188–C196 (2011).
5. B. Mangote, L. Gallais, M. Commandré, M. Mende, L. Jensen, H. Ehlers, M. Jupé, D. Ristau, A. Melninkaitis, J. Mirauskas, V. Sirutkaitis, S. Kičas, T. Tolenis, and R. Drazdys, "Femtosecond laser damage resistance of oxide and mixture oxide optical coatings," *Opt. Lett.* **37**(9), 1478–1480 (2012).
6. M. Mende, S. Schrameyer, H. Ehlers, D. Ristau, and L. Gallais, "Laser damage resistance of ion-beam sputtered Sc₂O₃/SiO₂ mixture optical coatings," *Appl. Opt.* **52**(7), 1368–1376 (2013).
7. T. Eidam, S. Hanf, E. Seise, T. V. Andersen, T. Gabler, C. Wirth, T. Schreiber, J. Limpert, and A. Tünnermann, "Femtosecond fiber CPA system emitting 830 W average output power," *Opt. Lett.* **35**(2), 94–96 (2010).
8. P. Russbueltd, T. Mans, J. Weitenberg, H. D. Hoffmann, and R. Poprawe, "Compact diode-pumped 1.1 kW Yb:YAG Innoslab femtosecond amplifier," *Opt. Lett.* **35**(24), 4169–4171 (2010).
9. M. Schulz, R. Riedel, A. Willner, T. Mans, C. Schnitzler, P. Russbueltd, J. Dolkemeyer, E. Seise, T. Gottschall, S. Hädrich, S. Duesterer, H. Schlarb, J. Feldhaus, J. Limpert, B. Faatz, A. Tünnermann, J. Rossbach, M. Drescher, and F. Tavella, "Yb:YAG Innoslab amplifier: efficient high repetition rate subpicosecond pumping system for optical parametric chirped pulse amplification," *Opt. Lett.* **36**(13), 2456–2458 (2011).
10. C. J. Saraceno, F. Emaury, O. H. Heckl, C. R. E. Baer, M. Hoffmann, C. Schriber, M. Golling, T. Südmeier, and U. Keller, "275 W average output power from a femtosecond thin disk oscillator operated in a vacuum environment," *Opt. Express* **20**(21), 23535–23541 (2012).
11. D. Bauer, I. Zawischa, D. H. Sutter, A. Killi, and T. Dekorsy, "Mode-locked Yb:YAG thin-disk oscillator with 41 μJ pulse energy at 145 W average infrared power and high power frequency conversion," *Opt. Express* **20**(9), 9698–9704 (2012).

12. O. Pronin, J. Brons, C. Grasse, V. Pervak, G. Boehm, M.-C. Amann, V. L. Kalashnikov, A. Apolonski, and F. Krausz, "High-power 200 fs Kerr-lens mode-locked Yb:YAG thin-disk oscillator," *Opt. Lett.* **36**(24), 4746–4748 (2011).
13. T. Metzger, A. Schwarz, C. Y. Teisset, D. Sutter, A. Killi, R. Kienberger, and F. Krausz, "High-repetition-rate picosecond pump laser based on a Yb:YAG disk amplifier for optical parametric amplification," *Opt. Lett.* **34**(14), 2123–2125 (2009).
14. S. Klingebiel, C. Wandt, C. Skrobol, I. Ahmad, S. A. Trushin, Z. Major, F. Krausz, and S. Karsch, "High energy picosecond Yb:YAG CPA system at 10 Hz repetition rate for pumping optical parametric amplifiers," *Opt. Express* **19**(6), 5357–5363 (2011).
15. I. Pupeza, T. Eidam, J. Rauschenberger, B. Bernhardt, A. Ozawa, E. Fill, A. Apolonski, T. Udem, J. Limpert, Z. A. Alahmed, A. M. Azzeer, A. Tünnermann, T. W. Hänsch, and F. Krausz, "Power scaling of a high-repetition-rate enhancement cavity," *Opt. Lett.* **35**(12), 2052–2054 (2010).
16. I. Pupeza, S. Holzberger, T. Eidam, H. Carstens, D. Esser, J. Weitenberg, P. Rußbüldt, J. Rauschenberger, J. Limpert, T. Udem, A. Tünnermann, T. W. Hänsch, A. Apolonski, F. Krausz, and E. Fill, "Compact high-repetition-rate source of coherent 100 eV radiation," *Nat. Photonics* **7**(8), 608–612 (2013).
17. H. Carstens, S. Holzberger, J. Kaster, J. Weitenberg, V. Pervak, A. Apolonski, E. Fill, F. Krausz, and I. Pupeza, "Large-mode enhancement cavities," *Opt. Express* **21**(9), 11606–11617 (2013).
18. *ISO 11551: Test Method for Absorbance of Optical Laser Components*, International Organization for Standardization, Technical Committee (International Standard, 1997).
19. A. O'Keefe and D. A. G. Deacon, "Cavity ring-down optical spectrometer for absorption measurements using pulsed laser sources," *Rev. Sci. Instrum.* **59**(12), 2544–2551 (1988).
20. A. V. Tikhonravov and M. K. Trubetskov, "OptiLayer software," <http://www.optilayer.com>.
21. J. H. Apfel, "Optical coating design with reduced electric field intensity," *Appl. Opt.* **16**(7), 1880–1885 (1977).
22. H. Fattahi, C. Y. Teisset, O. Pronin, A. Sugita, R. Graf, V. Pervak, X. Gu, T. Metzger, Z. Major, F. Krausz, and A. Apolonski, "Pump-seed synchronization for MHz repetition rate, high-power optical parametric chirped pulse amplification," *Opt. Express* **20**(9), 9833–9840 (2012).
23. A. Rosenfeld, M. Lorenz, R. Stoian, and D. Ashkenasi, "Ultrashort-laser-pulse damage threshold of transparent materials and the role of incubation," *Appl. Phys. Mater. Sci. Process.* **69**(7), S373–S376 (1999).
24. A. Melnikaitis, J. Mirauskas, and V. Sirutkaitis, "Adaptive laser-induced damage detection," *Proc. SPIE* **7504**, 75041F (2009).
25. M. Mero, D. Ristau, J. Krüger, S. Martin, K. Starke, B. Clapp, J. Jasapara, W. Kautek, and W. Rudolph, "On the damage behavior of dielectric films when illuminated with multiple femtosecond laser pulses," *Opt. Eng.* **44**(5), 051107 (2005).
26. B. C. Stuart, M. D. Feit, S. Herman, A. M. Rubenchik, B. W. Shore, and M. D. Perry, "Nanosecond-to-femtosecond laser-induced breakdown in dielectrics," *Phys. Rev. B Condens. Matter* **53**(4), 1749–1761 (1996).
27. *Handbook of Ellipsometry* (William Andrew, 2005).
28. V. Mikhelashvili and G. Eisenstein, "Optical and electrical characterization of the electron beam gun evaporated TiO₂ film," *Microelectron. Reliab.* **41**(7), 1057–1061 (2001).

1. Introduction

The weakest parts of ultrafast laser systems with respect to laser-induced damage are often optical multilayer mirrors. This fact has motivated extensive studies of ultrashort-pulse-induced optical breakdown of thin-films over the last decade [1–6]. All of them have been carried out by measuring the damage threshold at a low average power, either in single-shot mode or by using a pulse train at a kHz repetition rate.

However, recently developed oscillators and amplifiers, based on fiber [7], innoslab [8,9], and thin-disk technology [10–12], are capable of generating subpicosecond pulses with energies of several tens of μJ at repetition rates of more than 10 MHz, resulting in several hundreds of watts of average output power and multiple megawatts of peak power. Optical damage is among the challenges towards scaling up the power of such systems. Moreover, their output is often intensified further in regenerative amplifiers [13], optical parametric amplification (OPA) stages [14], and inside enhancement cavities [15,16]. The latter can reach average intracavity power of several tens of kW, which is limited by the damage threshold of optical coatings [15,17].

The straightforward way to deal with optical breakdown is to increase the beam size. However, that requires larger optics and increases the overall footprint of the system, hence the costs rise substantially. In addition, the larger the size of the optics, the more difficult it becomes to provide uniform surface quality. Furthermore, the damage threshold of the whole optical element is as low as the damage threshold of its weakest spot. Thus, before undertaking the approach of increasing the size of the optical components, it would be beneficial first to try to increase their damage threshold. It is essential, therefore, to study the

ultrafast damage behavior of thin-films not only in the single-shot and kHz repetition rate regimes, but also for MHz repetition rates at high average power.

In this work we explore the dependence of MHz ultrashort pulse damage threshold of multilayer thin-films on the band gap and on the electric field distribution. We demonstrate that by suppressing the electric field in high-index layers and shifting its maxima to low-index layers the damage threshold can be increased by 30%. A criterion for optimal electric field distribution is also given.

2. Materials

We investigated the laser-induced damage of three different sets of samples. All of them were multilayer thin-film compositions, where SiO_2 was used as the low-index material in each coating and the high-index material was TiO_2 , Ta_2O_5 , HfO_2 , or Al_2O_3 .

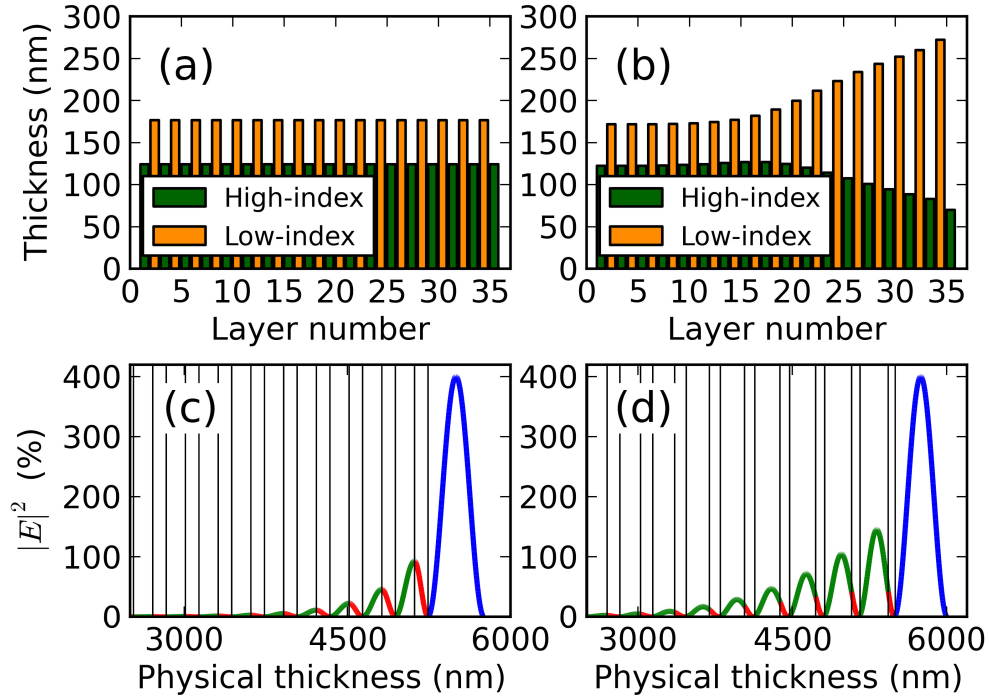


Fig. 1. (a) and (b): Layer thickness profile of a QWOT stack of $\text{Ta}_2\text{O}_5/\text{SiO}_2$ (a) and of a layer stack of $\text{Ta}_2\text{O}_5/\text{SiO}_2$ with reduced electric field intensity (EFI) inside the Ta_2O_5 layers (b). (c) and (d): Electric field distributions inside of (a) and (b), respectively. The electric field inside L and H layers is represented accordingly by green and red sections, whereas the field in the incident medium is colored in blue.

The first set consisted of quarter-wave optical thickness (QWOT) stacks made using SiO_2 and one of each of the aforementioned high-index materials. These layer stacks are represented by the formula $(HL)^m H$, where $m=17$, and H and L denote high- and low-index layers, respectively. The layer thickness profile of this 35-layer QWOT stack of $\text{Ta}_2\text{O}_5/\text{SiO}_2$ is given in Fig. 1(a) and the electric field distribution inside such stack is given in Fig. 1(c). The absorption of the samples from this set was measured using a calorimetric approach [18], whereas their total losses were measured using a cavity ring-down technique [19]. The results from these measurements are shown in Fig. 2.

The second set contained narrow band-pass (NBP) 33-layer filters described by the formula $(HL)^n 2H(LH)^n$, where $n=8$. The only difference between the QWOT stacks and the NBP filters was a cavity high-index layer in the middle of the stack with half-wave optical

thickness. At the central wavelength the electric field inside the cavity layer is significantly enhanced. Therefore, these NBP samples were expected to have lower damage threshold than the QWOT stacks made of the same pair of materials.

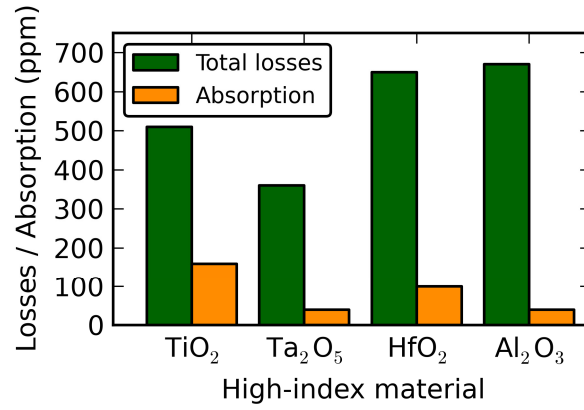


Fig. 2. Absorption and total losses of the QWOT stacks, on which damage threshold measurements were performed.

The samples in the third set were designed in such way that the electric field within the high-index layers was suppressed and its maxima were shifted to the low-index layers (Fig. 1(d)). Dielectric thin-film structure with such electric field distribution was expected to have higher damage threshold than a QWOT, since materials of lower refractive index have broader band gap and previous studies in the ultrashort regime have shown that the breakdown threshold of dielectrics scales with their band gap [2]. The design of these coatings with optimized electric field intensity (EFI) was found numerically by using the commercially available software OptiLayer [20]. The resulting layer thickness profile is displayed in Fig. 1(b) and its electric field distribution is depicted in Fig. 1(d). The obtained EFI design was rather similar to another one, which was retrieved by an analytical approach to the same problem [21].

All samples were prepared using electron beam evaporation. The only exception was the QWOT stack of Al₂O₃/SiO₂, which was deposited using magnetron sputtering technique.

3. Experimental setup

In order to explore the ultrafast damage behavior of multilayer thin-films at MHz repetition rate and high average power, we used a mode-locked Yb:YAG thin-disk oscillator operating at wavelength of 1030 nm and repetition rate of 11.5 MHz. It delivered pulses with energy of 5 μ J and duration of about 1 ps. The laser system is described in more detail in [22].

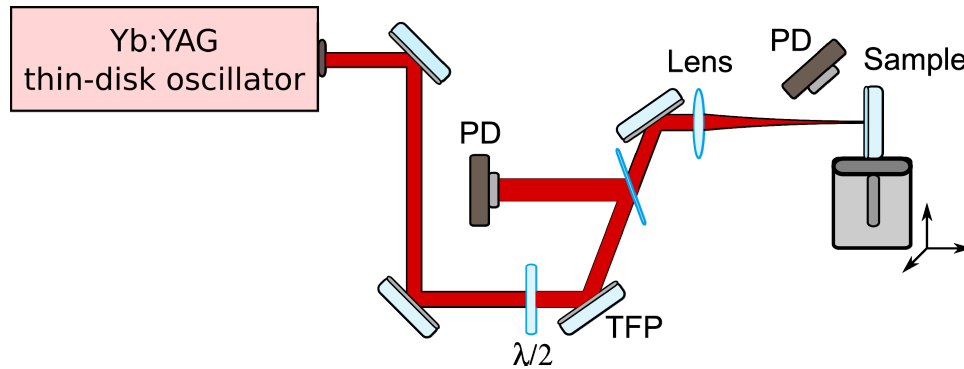


Fig. 3. Measurement setup: PD – photodiode, $\lambda/2$ – half-wave plate, TFP – thin-film polarizer.

The setup used for damage threshold measurements is depicted in Fig. 3. The intensity of the incoming beam was controlled by rotating a half-wave plate mounted on a motorized stage and a thin-film polarizer. A small portion of the beam was deflected to a calibrated photodiode, allowing us to measure *in situ* the incident power. The main part of the beam was focused on the sample down to 25 μm in diameter measured at level $1/e^2$ from the peak intensity, using antireflection coated spherical lens with 70 mm focal length. The sample was mounted on a motorized three dimensional translation stage. A second photodiode was placed near the sample to monitor the light scattered off its surface. An abrupt change in the scattering behavior of the sample was used as an indicator of damage. This method has been applied successfully in the past [23,24] and is one of the damage detection methods recommended by ISO 21254:2011.

The sample was placed in the focal plane of the laser beam in such way that an undamaged site was irradiated and the light scattered off the sample was monitored for a certain time interval (typically a second). Then the fluence was increased and the scattered light was measured again for the same period of time, while illuminating the same spot on the sample. That routine was iterated to cover a certain fluence range, within which the damage threshold lay. The damage threshold was defined as the fluence at which the behavior of scattering signal with respect to laser fluence changed rapidly. A typical recording of scattering signal as a function of laser fluence is given in Fig. 4. The fluence value after which the scattering signal starts to grow rapidly defines the damage threshold fluence.

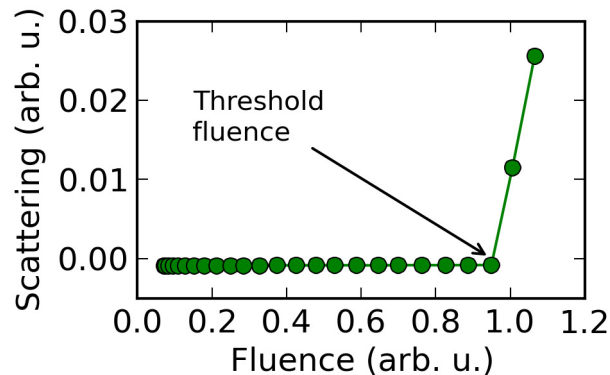


Fig. 4. Scattering signal versus fluence: example damage threshold measurement. The arrow points to the fluence at which damage occurred.

It is worth noting that the measurement procedure described in the previous paragraph differs from the recommended by ISO 21254:2011, where the laser beam is positioned on a separate site on the sample for each fluence value. This is done in order to avoid various incubation effects [25]. Since in our case more than 11 million pulses hit the sample each second and incubation effects are part of the damage process anyway, for the sake of simplicity we chose not to comply with ISO 21254:2011. However, the detailed description of the measurement procedure and the setup allows the reproduction of the obtained results.

4. Results and discussion

It has been shown previously that for pulse durations τ below ten picoseconds the laser-induced damage in dielectrics departs from being thermally-dominated and is instead initiated by a combination of multiphoton, tunneling, and avalanche ionization mechanisms [26]. Therefore, in this work we refer to pulses shorter than 10 ps as ultrashort pulses.

In the ultrashort pulse regime, the damage threshold was found to scale linearly with the band gap of the material [2]. On the other hand, for materials with negligible absorption the real part of the dielectric function, i.e., the refractive index, is inversely proportional to the

band gap [27]. Therefore, one can expect that the damage threshold of a QWOT stack is constrained by the breakdown threshold of its high-index material.

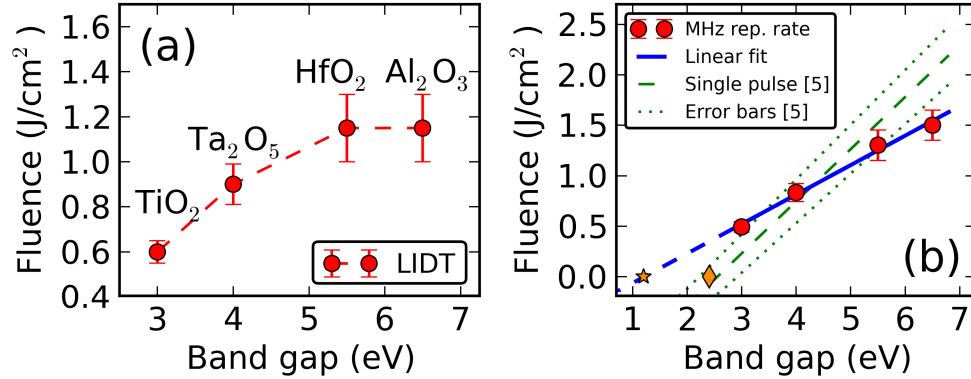


Fig. 5. Damage fluences of different QWOT stacks versus band gap of the respective high-index materials. The measured damage fluences of the samples do not scale linearly with the band gap (a). However, if the electric field distribution inside of the QWOT stacks is taken into account (b), the “internal” damage fluences were found to follow a linear dependence on the band gap (blue line). The green dashed line represents the corrected band gap dependence reported in [5] for single pulse measurements with 500 fs pulses at 1030 nm (see text for details). The star and the diamond mark the photon energies at 1030 nm and 515 nm, respectively.

Figure 5(a) displays the damage threshold fluence of QWOT stacks employing different high-index materials versus the band gap of the respective material. The error bars represent experimental error of 10% for the obtained damage threshold values. The band gaps of Ta₂O₅, HfO₂, and Al₂O₃ were taken from [5], whereas the band gap of TiO₂ was found in [28]. Evidently, even though the breakdown threshold of a quarter-wave stack scales to some extent with the band gap of its high-index material, the dependence is nonlinear. Note, however, that these fluence values were calculated at the front surface of the sample, without taking into account the electric field distribution inside the QWOT stack [Fig. 1(c)]. If we take that into consideration, we will obtain threshold fluence values which are characteristic for the layers themselves. We call this “internal” threshold fluence for layer X :

$$F_{int}^X = \left| E_{max}^X / E_{inc} \right|^2 F_{ext}. \quad (1)$$

Here F_{ext} is the measured threshold fluence on the front surface of the sample, E_{inc} is the magnitude of the incident electric field, and E_{max}^X is the magnitude of the maximal electric field inside layer X .

In the case of QWOT stacks, where the peaks of electric field are positioned on the boundaries between layers [Fig. 1(c)], the limiting factor is the internal damage threshold of high-index layers F_{int}^H , because of their narrower band gap compared to low-index layers. In addition, it can be shown by writing the characterization matrix for a QWOT stack that, at normal incidence, the height of the peak on the first boundary between H and L layers is inversely proportional to the square of the refractive index of the H material. After we make a correction in accordance with Eq. (1) and with respect to the high-index layer, plotting the internal threshold fluence versus the band gap of the high-index material reveals a clear linear dependence [Fig. 5(b)].

A couple of observations can be made here. First, it is evident that although the damage threshold does depend on the band gap of the material [Fig. 5(b)], there is a certain point beyond which the damage threshold of the whole QWOT stack [Fig. 5(a)] cannot be increased any more merely by choosing a high-index material with a broader band gap.

Second, even though the different samples absorbed different amount of the incident light, in some cases by a factor of four [Fig. 2], a linear scaling of the damage threshold with respect to the band gap of the high-index material could be observed. This is a strong indication that even at MHz repetition rates and at large average power (some tens of watts), thermal effects do not constitute an important part of the damage mechanism in the ultrashort pulse regime ($\tau < 10$ ps).

Ideally, we would like to compare the damage threshold values obtained at 11 MHz repetition rate with ones retrieved by using a laser beam with a kHz repetition rate and otherwise similar parameters to ours (i.e., wavelength, pulse duration, and focal spot size). However, to the best of our knowledge, currently no study exists on the kHz ultrashort-pulse LIDT at 1030 nm of the materials examined here. Therefore, we weigh our results against the ones reported in [5] for single 500 fs pulses at 1030 nm. To make a fair comparison, we modified the results from [5] in two aspects: (i) to compensate for the difference in pulse duration by using the τ^k law, where $k = 0.3$ [2]; (ii) to account for measuring the LIDT of infinitely many pulses (more than 10^6), which has been found to be equal to about two thirds of the single pulse damage [25]. The linear dependence reported in [5] modified in such way is depicted as green dashed line in Fig. 5(b); the green dotted lines represent the respective error bars. Although our measurements are in a relatively good quantitative agreement with the so-modified results from [5], they clearly follow a different trend [Fig. 5(b)].

An interesting fact to point out is that the linear dependence obtained for 11 MHz crosses the abscissa at 1.2 eV, which is close to the photon energy at 1030 nm (denoted with a star in Fig. 5(b)). On the other hand, the photon energy at 515 nm ($= 1030/2$ nm) is 2.4 eV (marked with a diamond in Fig. 5(b)), which is within the error bar of the point where the linear band-gap dependence reported in [5] crosses the abscissa (2.56 eV). Further investigation is required to determine whether these observations have any physical meaning.

The comparison of the damage threshold values of QWOT stacks with the corresponding threshold values of the NBP filters is given in Fig. 6. As explained in Section 2, there is a field enhancement inside the cavity high-index layer of the NBP filter. As illustrated in Fig. 6, the damage threshold of such coating is lower than that of a QWOT stack with the same high-index material. This provides additional evidence that the distribution of electric field inside the multilayer coating plays an important role in determining its optical resistance.

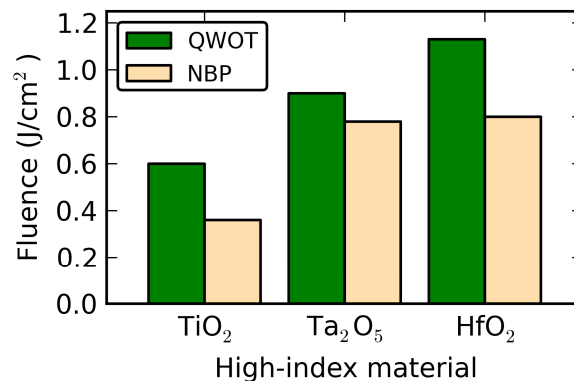


Fig. 6. Comparison of the damage threshold values of QWOT stacks employing different high-index materials with the respective narrow band-pass (NBP) filters.

It should be noted that due to high sensitivity to deposition errors of the NBP design, the actual distribution of electric field inside the produced coating may deviate substantially from the theoretical one. Thus, no efforts were made to estimate the internal damage fluence of these coatings in analogy to Fig. 5(b) and according to Eq. (1). Nevertheless, Fig. 6 provides evidence that the damage threshold of dielectric stacks at pulse durations of 1 ps is dependent

on the electric field distribution even at high average power. We explored that dependency to find out whether it can be exploited to improve the damage threshold of high reflective coatings and to what extent.

Since in the ultrashort pulse regime the damage behavior of thin-films is mainly dictated by intrinsic material properties [2], the damage threshold itself can also be regarded as an intrinsic property of the thin-film material at a particular combination of wavelength and pulse duration. That is, an assumption can be made that the threshold fluence of the high-index material F_{int}^H is a characteristic property of that material and is not dependent on defects and impurities. Of course, the same also holds for the threshold fluence of the low-index material F_{int}^L . From that and from Eq. (1) it follows that the damage threshold of the whole thin-film stack F_{ext} is governed by

$$F_{ext} = \min \left(\left| E_{inc} / E_{max}^H \right|^2 F_{int}^H, \left| E_{inc} / E_{max}^L \right|^2 F_{int}^L \right), \quad (2)$$

where E_{max}^L is the magnitude of maximum electric field in the low-index material. This expression implies also that if the electric field inside the high-index material is low enough, the electric field inside the low-index material becomes the limiting factor. One can see from Eq. (2) that the damage fluence of the assembly F_{ext} has maximum when

$$\left| E_{max}^H / E_{max}^L \right|^2 = F_{int}^H / F_{int}^L. \quad (3)$$

To verify that experimentally we prepared coatings optimized for electric field distribution (EFI). A typical EFI design is given in Fig. 1(b) and the corresponding field distribution is shown in Fig. 1(d). Samples with such designs were manufactured using TiO_2 and Ta_2O_5 as high-index materials and their damage thresholds are compared with QWOT stacks of the respective materials in Fig. 7(a). In both cases an improvement of about 30% was obtained.

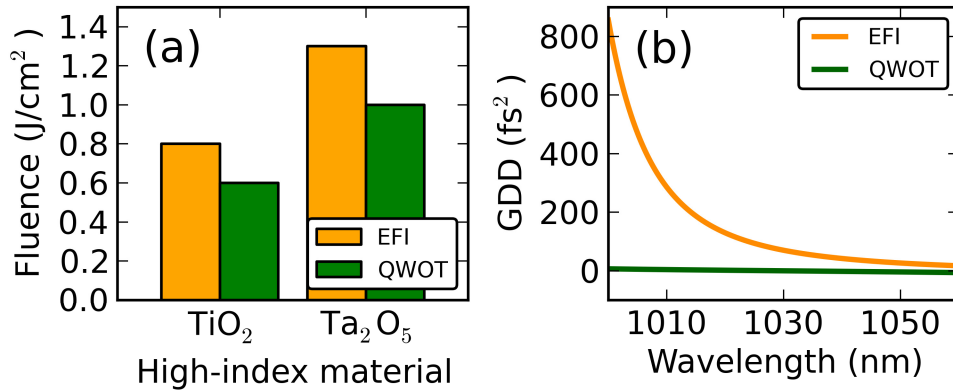


Fig. 7. Comparisons between a QWOT stack and an EFI stack with respect to: (a) damage threshold of compositions of different materials; (b) theoretical group delay dispersion (GDD) around the central wavelength.

On the downside, however, the dispersion properties of the EFI designs are very unfavorable to ultrashort pulses, as such coatings would introduce a relatively large amount of group delay dispersion, as well as dispersion of higher orders [Fig. 7(b)]. These will lead to pulse broadening and the formation of sideband pulses, respectively.

5. Conclusion

We have investigated the damage threshold of three different types of coatings made with TiO_2 , Ta_2O_5 , HfO_2 , or Al_2O_3 as high-index material and SiO_2 as low-index material. The measurements were carried out using a mode-locked Yb:YAG thin-disk oscillator generating at central wavelength of 1030 nm pulses with duration of 1 ps and energy of 5 μJ at a repetition rate of 11.5 MHz, resulting in 55 W average power.

We have shown that the damage fluence of quarter-wave stacks scales linearly with the band gap of the used high-index material if the damage threshold is normalized with respect to electric field. This suggests that thermal effects do not play a significant part in the ultrashort pulse damage mechanism even at MHz repetition rates and at high average powers. Further proof of the significance of the electric field distribution is given by NBP filter stacks, where the electric field inside a high-index layer was enhanced, thus reducing the damage threshold of these structures. This dependence on electric field was exploited to produce highly reflective coatings with higher optical resistance by suppressing the electric field inside high-index materials and shifting its maxima to the low index materials. Additionally, a condition for optimal field suppression was also given.

Acknowledgments

This work was supported by the Cluster of Excellence “Munich-Centre for Advanced Photonics” (<http://www.munich-photonics.de/>) of the German Research Foundation (DFG). The authors also thank Oleg Pronin for initial technical support and Olga Razskazovskaya for her help with preparation of the samples.